The Laticyclic [2 + 2 + 2] Conjugation: PE and UV Spectroscopical Investigation of the Interaction Between Three Parallel π Bonds[1)]

Siegfried Hünig*[b], Hans-Dieter Martin*[a], Bernhard Mayer[a], Karl Peters[c], Frank Prokschy[b], Michael Schmitt[b], and Hans Georg von Schnering*[c]

Institut für Organische Chemie I, Universität Düsseldorf[a],
Universitätsstraße 1, D-4000 Düsseldorf

Institut für Organische Chemie, Universität Würzburg[b],
Am Hubland, D-8700 Würzburg

Max-Planck-Institut für Festkörperforschung[c],
Heisenbergstraße 1, D-7000 Stuttgart 80

Received September 1, 1986

Azo compound **1** contains three parallel π bonds which can give rise to a laticyclic [2 + 2 + 2] conjugation. Experimental evidence for that is obtained from photoelectron spectra of **1** and the related compounds **2**, **3**, and **5**. Geometry optimizations by means of the semiempirical MNDO method predicts a smaller distance (by 7 pm) for $d(\pi_{NN}-\pi^5_{CC})$ than for $d(\pi_{NN}-\pi^6_{CC})$ which is confirmed by X-ray structure determination. The consequences of this laticyclic conjugation for the photochemical reactivity are investigated, and reasons are given for the preferential cycloaddition of the azo group to the π^5_{CC} double bond.

Die laticyclische [2 + 2 + 2]-Konjugation: PE- und UV-spektroskopische Untersuchung der Wechselwirkung zwischen drei parallelen π-Bindungen[1)]

Die Azoverbindung **1** enthält drei parallel angeordnete π-Bindungen, die zu einer laticyclischen [2 + 2 + 2]-Konjugation Anlaß geben können. Experimentelle Hinweise dafür werden aus den Photoelektronenspektren von **1** und den verwandten Verbindungen **2**, **3** und **5** erhalten. Geometrieoptimierungen mit Hilfe der semiempirischen MNDO-Methode berechnen für $d(\pi_{NN}-\pi^5_{CC})$ einen um 7 pm kleineren Abstand als für $d(\pi_{NN}-\pi^6_{CC})$. Dies wird durch die Röntgenstrukturanalyse von **1** bestätigt. Die Konsequenzen dieser laticyclischen Konjugation für die photochemische Reaktivität werden untersucht, und es werden Gründe für die bevorzugte Cycloaddition der Azogruppe mit der π^5_{CC}-Doppelbindung genannt.

In 1971 Goldstein and Hoffmann[2)] described – as they called it – novel and modified Hückel rules with the help of which the electronic stabilization of three-dimensional topologies can generally be predicted. For the parallel π bonds two extreme cases my be discussed within the scope of this model. Due to their symmetry and their interaction diagrams they show a significant difference (Figure 1).

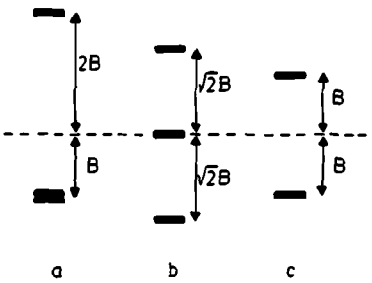

Figure 1. Interaction diagram for three parallel π bonds in a) longicyclic (D_{3h}) and b) laticyclic (D_{3h}) topology and c) comparison with the split of two π bonds. $B = \langle\pi|H|\pi\rangle$ is the interaction parameter between the π-MO's

The best-known example for a homoconjugation of type a (Figure 1) is barrelene[3)]. Hardly any examples are known for type b and, as far as we know, no quantitative investigations exist.

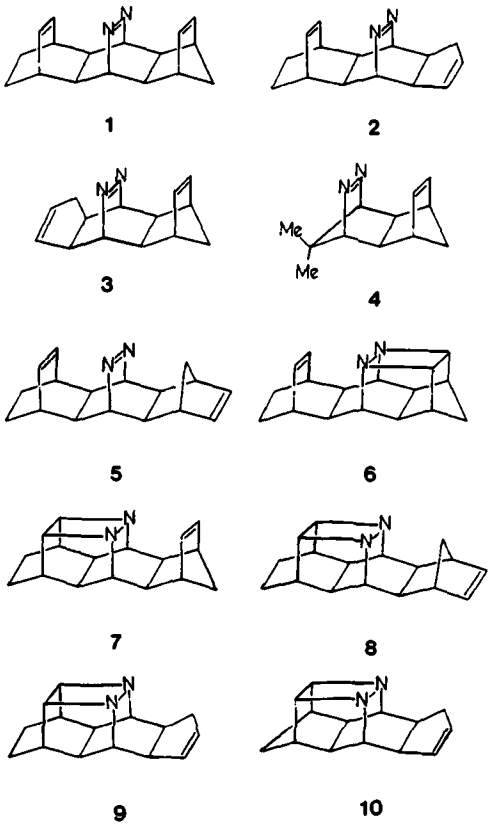

  0009–2940/87/0202–0195 $ 02.50/0

Yet, Hünig and Prokschy[4a] recently synthesized the diazatriene **1**, which might show laticyclic conjugation in contrast to the azo compounds **2**[4a] and **3**[4b].

In **2** or **3**, respectively, geometry and asymmetry prevent such a conjugation, only the considerable homoconjugation between the two parallel π bonds in **3** could be proved spectroscopically[5] as well as by photolysis[4c]. Therefore, it was of great interest to show whether that special and comparatively rare type of conjugation does exist in **1** and whether the theoretically expected larger split (Figure 1b) compared to the interaction between only two π bonds as in the compounds **2**, **3**, or **4**[6] could be proved experimentally. We now want to report on comparative PE and UV investigations of **1**, **2**, **3**[5], and **5**.

PE and UV Spectra

Figure 2 shows the He(I) spectra of **1**, **2**, **3**, and **5**. The ionization energies are listed in Table 1 and the UV excitation energies are given in Table 2.

Table 1. Vertical ionization energies of **1**–**3**[5] and **5** (in eV, estimated error: ±0.03). Values in parentheses are uncertain

	$I_{m,1}$	$I_{m,2}$	$I_{m,3}$	$I_{m,4}$	$I_{m,5}$
1	7.95	8.40	8.85	(10.0)	(10.3)
2	8.05	8.85	9.10	(10.1)	(10.4)
3	7.90	8.65	9.10	10.15	10.60
5	7.88	8.75	9.02	9.85	10.15

Discussion of the PE Spectra

Empirical Correlations and LCBO Model

The PE spectra of **1**–**3** and **5** show three similar bands between 7.5 and 10.0 eV. A relatively broad but less intensive ionization event at about 7.9–8.0 eV is followed by two more intensive bands, of which the first one lies between 8.4 and 8.7 eV and the second one between 8.8 and 9.10 eV. In all three compounds the first ionization at about 8.0 eV is ascribed to the n_-^{-1} process. The comparatively constant location of this band can be attributed to a lower sensitivity to proximity effects. This is typical for n_- orbitals which show hardly any overlap with neighbouring π orbitals, because of their localization in the C–N=N–C plane.

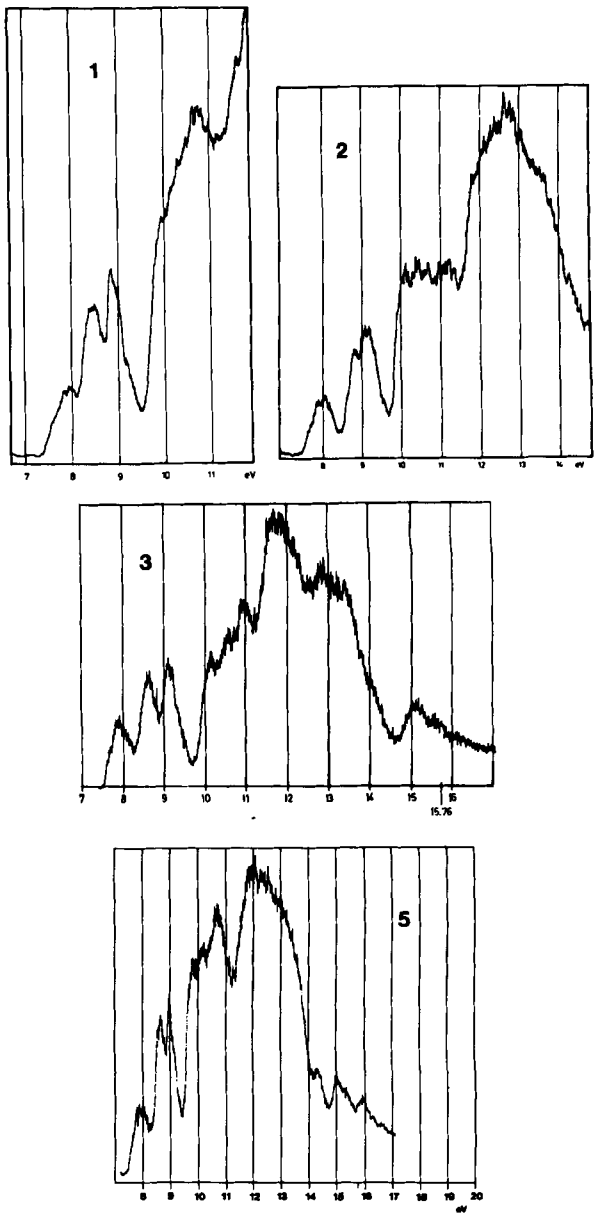

Figure 2. He(I) photoelectron spectra of **1**, **2**, **3**, and **5**

The most significant differences in the spectra of **1**–**3** and **5** can be seen in the two π_{CC} bands. **1** deviates most, whereas **2**, **3**, and **5** show great similarity. **2** as well as **3** display an

Table 2. UV Absorption data of azo compounds **1**, **3**, and **5**

Compound	Solvent	π–π*			n–π* (λ_{max} (ε) [nm])
1	*n*-Hexane		sh 240(900)		398(160), sh 389(100), sh 358(20)
	CH_3CN		247(900)		395(120), sh 386(90), sh 357(30)
	EtOH		252(700)		388(70), sh 374(60), sh 348(35)
		ε_{270}	ε_{250}	ε_{230}	
3	*n*-Hexane	100	290	955	395(110), sh 386(70), sh 356(20)
	CH_3CN	130	290	745	394(100), sh 384(70), sh 355(20)
	EtOH	235	400	625	388(70), sh 378(60), sh 352(30)
5	*n*-Hexane	65	285	720	397(105), sh 387(65), sh 357(20)
	CH_3CN	90	285	565	396(80), sh 384(55), sh 356(20)
	EtOH	150	310	480	388(50), sh 377(45), sh 352(20)

ionization event at 9.1 eV. Since both polycycles have the cyclopentene fragment in common, I_m = 9.1 eV can obviously be ascribed to the π_{CC} cyclopentene orbital. The π electrons of cyclopentene ionize at exactly the same value. Therefore, the band at 8.85 eV or 8.65 eV of **2** or **3**, respectively, originates from the π electrons of the bicyclo[2.2.2]octene or the bicyclo[2.2.1]heptene fragment, respectively. Compared to the known values of bicyclo[2.2.2]octene (9.05 eV)[7] and bicyclo[2.2.1]heptene (8.97 eV)[7] these ionization energies are destabilized by 0.20 eV or 0.32 eV, respectively, which can be explained by the homoconjugative influence of the π_{NN} orbital[5]. From the basis energies $\varepsilon(\pi_{CC})$ = −8.9 eV for **3**, $\varepsilon(\pi_{CC})$ = −9.05 eV for **2** and $\varepsilon(\pi_{NN})$ = −10.4 eV[5] and the measured ionization energies [$I_m(\pi_{NN})$ is supposed to be 10.6 eV in both cases] an effective interaction parameter H_{eff} = $\langle\pi_{CC}|H|\pi_{NN}\rangle$ of −0.62 eV for **3** and −0.56 eV for **2** can be calculated. For compound **4** only an approximate value $H_{eff} \approx -0.8$ eV could be given, since the π_{NN} ionization energy could not exactly be ascertained. The spectrum of **1** is most remarkable: $I_{m,3}(\mathbf{1}) = I_{m,2}(\mathbf{2})$, but $I_{m,2}(\mathbf{1}) < I_{m,2}(\mathbf{3})$, i.e., whereas the ionization energies of the π electrons of the bicyclo[2.2.2]octene fragments in **1** and **2** are equal, the π_{CC} orbital of the norbornene fragment in **1** is destabilized compared with the corresponding orbital energy of **3**!

This observation may be explained with a laticyclic conjugation (Figure 1b). Given exactly the same interaction parameter B the three levels in Figure 1b display a larger split ($2\sqrt{2}\,B$) than in the case of 1c (2B). Figure 3 presents the situation of the π-MO's of **1** realistically within the Hückel model. The above-deduced parameters H_{eff} allow us to compare the simple homoconjugation ($\pi_{NN}-\pi_{CC}$) with the laticyclic conjugation ($\pi_{CC}-\pi_{NN}-\pi_{CC}$). The latter interaction leads to a stronger destabilization of ε_1 in **1** than it is the case in **2** or **3** (8.57 < 8.67 < 8.84).

Further support for this interpretation is given by the spectrum of **5**. In **5** the norbornene moiety is folded down and the interaction with this fragment is therefore switched off. The result is a normal norbornene π ionization energy (9.02 eV) and a destabilized π energy (8.75 eV) of the bicyclo[2.2.2]octene unit similar to that found in **2**. Since inductive and through-bond effects on the norbornene fragment in **1** and **5** should be identical, this sizeable difference in the norbornene π ionization energies (9.02 eV in **5**, 8.40 eV in **1**) demonstrates once more the result of the laticyclic conjugation in **1**.

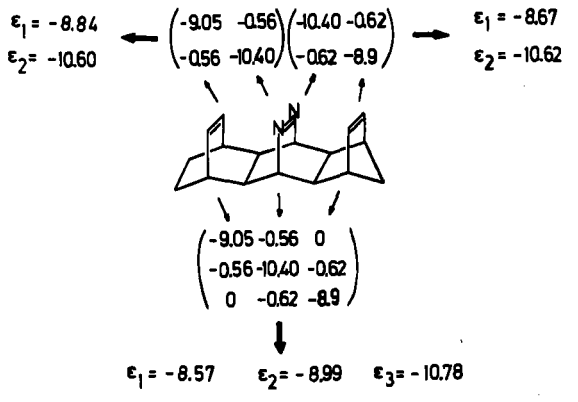

Figure 3. HMO model of the laticyclic conjugation in **1**. All values are given in eV. The sequence of the matrix elements corresponds to the arrangement of the π bonds in the molecule. Above the molecule: fragmentary interactions $\pi_{NN}-\pi_{CC}$. Below the molecule: laticyclic conjugation $\pi_{CC}-\pi_{NN}-\pi_{CC}$. Basis energies and H_{eff} as described in the text

MO Calculations

The geometry of **1** was optimized with the help of the MNDO model[8], since that method yields good results relating to the transanular distances in isodrins[5,6]. For a comparison the force field model MMI[9] with the parameters by J. P. Snyder[10] was used as well. The following values were found for the transanular distances between the azo group and the π bonds π^5_{CC} (norbornene) or π^6_{CC} (bicyclo[2.2.2]octene), respectively: MNDO, $d(\pi_{NN}-\pi^5_{CC})$ = 298 pm, $d(\pi_{NN}-\pi^6_{CC})$ = 305 pm; MM1, $d(\pi_{NN}-\pi^5_{CC})$ = 269 pm, $d(\pi_{NN}-\pi^6_{CC})$ = 274 pm. Both methods supply slightly larger values for the transanular distance between the azo group and the bicyclo[2.2.2]octene moiety. The SCF orbital energies obtained with MNDO geometries are given in Table 3.

Table 3. Comparison of orbital energies (in eV) of **1** with experimental values according to various methods

Orbital	Exp.	MNDO[8]	MINDO/3[11]	HAM/3[12]	STO-3G[13]
n_-	−7.95	−10.27	−8.25	−7.30	−7.07
π^5_{CC}	−8.40	−9.67	−8.84	−8.68	−7.34
π^6_{CC}	−8.85	−9.80	−9.21	−8.87	−7.72
$\Delta\pi$	0.45	0.13	0.37	0.19	0.38

MINDO/3[11], HAM/3[12], and STO-3G[13,14] methods give an orbital sequence which is in agreement with the empirical assignment.

Discussion of the UV Spectra and Photoreactivity

When irradiating **1** in chloroform with $\lambda > 320$ nm, predominantly a [2π + 2π] photocycloaddition between π_{NN} and π^5_{CC} takes place to yield **6**[4c]. The high chemoselectivity may have the following causes: a) The smaller distance $d(\pi_{NN}-\pi^5_{CC})$ favours the formation of this diazetidine, b) the first excited $^1n_-\pi^*$ state shows an increased bond order between π_{NN} and π^5_{CC}, c) the increase of strain energy for the formation of the two alternative diazetidines is smaller for **6** than for its isomer[15].

Although the strain energies for the diazetidines are not known, that reason for the selectivity is not considered important, since the difference in the strain energies for the two alternative photoreaction products should only be small. The arguments a and b seem to be more important. The calculated smaller atomic distance $d(\pi_{NN}-\pi^5_{CC})$ has been proved by X-ray structure analysis. The change of the $\pi_{NN}-\pi_{CC}$ bond order during $n_-\pi^*$ excitation is larger for the norbornene fragment than for the bicyclo[2.2.2]octene

unit. CNDO/S-CI[16] calculations do not only reproduce the observed wavelength adequately, they do also predict a change of bond order for the $^1n\_\pi^*$ state, which is larger in the direction of π^5_{CC} than in the direction of π^6_{CC}. The results of this calculation are illustrated in Figure 4. The HAM/3 calculation (without CI) yields a wavelength of λ = 370 nm (f = 0.001) for the n_π^* transition.

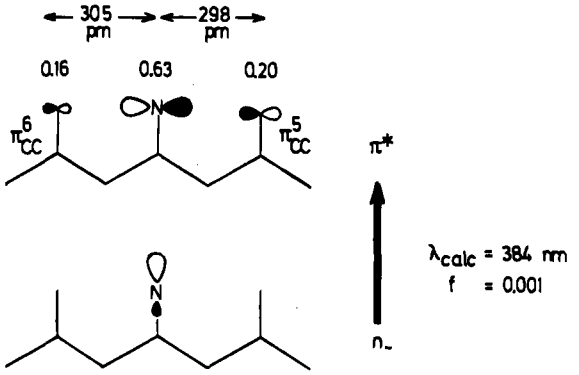

Figure 4. CNDO/S-CI calculation for 1. MNDO-optimized geometry; 40 singly excited configurations; CI expansion coefficient of the n_π^* configuration (π^* is LUMO): c = 0.86. The AO coefficients of π^* are given

On account of the SCF calculations the arguments a and b may be considered as the dominating reasons for the selectivity of the photoreaction **1**→**6**.

The UV spectroscopical data of azo compounds **1**, **3**, and **5** are given in Tab. 2. All compounds contain the same diazabicyclooctane moiety. The data are comparable to those of diazabicyclo[2.2.2]octane[17]. The $n\pi^*$ band of **1** shows a slight bathochromic shift compared with the reference compounds **2**, **3**, and **5** which allows us to conclude that there is a transanular $\pi_{NN}-\pi_{CC}$ interaction in **1** similar to compound **3**[5]. The blue shift of the absorption maximum with increasing polarity of the solvent confirms its assignment to the $n\pi^*$ transition.

Investigations on the $\pi\pi^*$ transition of bicyclic azo alkanes have not yet been described in literature. As a rule, this transition in azo compounds can only be observed as a maximum if it shows a bathochromic shift due to conjugation with a π system. For bicyclic azo alkanes a rising flank in the region of 200–250 nm can be found.

Compound **1** shows a shoulder in the short-wavelength range at 240 nm (hexane). This shoulder displays a bathochromic shift in more polar solvents, e.g. EtOH, and can then be observed as a maximum at 252 nm. In contrast to **1**, the compounds **3** and **5** show no such maximum but a rising flank. As is shown by the extinction coefficients for 270, 250, and 230 nm, given in Table 2, this flank does also display a bathochromic shift in polar solvents.

A red shift is characteristic for such $\pi\pi^*$ transitions whose excited state is more polar than the ground state. When taking the MO model as a basis for the $\pi\_\pi^*_\ddagger$ transition of **1** this transition proves to possess a partial charge transfer from π_{CC} to π_{NN}, which should be combined with a change in polarity.

As it was shown in Figure 4, the CNDO/S-CI method is very successful in calculating the weak n_π^* transition of **1**. It was therefore interesting to see whether the transition at shorter wavelengths (250 nm) might also be accounted for by this theoretical method. The CI calculation (40 singly excited configurations) indeed predicts a low-intensity $\pi\_\pi^*_\ddagger$ transition at 255 nm (f = 0.0006). The CI expansion coefficient of the $\pi\_\pi^*_\ddagger$ configuration is 0.99. In the CNDO model $\pi\_$ turns out to be the HOMO (0.32 p^6_{CC} + 0.21 p_{NN} + 0.48 p^5_{CC}), while $\pi^*_\ddagger$ represents the LUMO (0.16 p^6_{CC} − 0.63 p_{NN} + 0.20 p^5_{CC}). The excitation from the nonbonding SHOMO π_{nb} which is stronger localized on π^6_{CC} (0.53 p^6_{CC} − 0.35 p^5_{CC}) to $\pi^*_\ddagger$ takes place at even shorter wavelengths (230 nm, f = 0.0003). This second $\pi\pi^*$ transition is wholly dominated by the $\pi_{nb}\pi^*_\ddagger$ configuration, the CI expansion coefficient being 0.98. **1** therefore constitutes a second example[6] of an isodrin-type molecule where the low-intensity $\pi\_\pi^*_\ddagger$ transition can be separately observed.

Irradiations in Chloroform

According to ref.[4c] the azo compounds **1** and **5** are irradiated in $CDCl_3$ at a wavelength of $\lambda \geq$ 320 nm, and the

Table 4. Irradiation (Method A) of the azo compounds **1** and **5** in $CDCl_3$

Compound	Product	Yield (MPLC)
1 30 mg (0.12 mmol)	**6**:**7** (97:3, ^{1}H NMR)	83%
5 45 mg (0.18 mmol)	**8**	82%

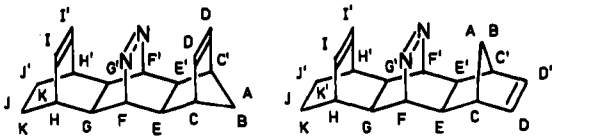

Table 5. Comparison of the ^{1}H-NMR data of the compounds **1**, **7**, and **8** relative to their norbornene (A–E′) or diazetidine (F–K′) moieties

	1		**7**		**8**
A,B	1.13, 1.24	– – –	(1.25 ?)[a]		1.21, 2.13
C,C′	2.73	– – –	2.85		2.75
D,D′	5.31[b]	– – –	6.09[b]		6.13
E,E′	2.34	– – –	2.45		1.74
F,F′	4.92		2.61	– – –	2.69
G,G′	2.02		2.31	– – –	2.31
H,H′	2.43		(1.78 ?)[c]	– – –	1.78
I,I′	5.66		(4.15 ?)[d]	– – –	4.17
J,J′[e]	1.40		1.90	– – –	1.90
K,K′[e]	1.08		1.48	– – –	1.45

[a] Presumably the expected AB multiplet is superimposed by the resonances of K,K′ of **6** at δ = 1.25. – [b] The same low-field shift (Δδ = 0.6 ppm) can be found for the protons I,I′ of **6** (δ = 6.22) compared to **1** (δ = 5.66). – [c] The resonances of the bridgehead protons H,H′ are probably superimposed by the signal of the methano bridge of **6** (δ = 1.78). – [d] Presumably superimposed by the signal of the corresponding diazetidine protons I,I′ of **6**. The comparison of **6** (δ = 4.15) and **8** (δ = 4.17) shows the small shift variance of these protons. – [e] This assignment is exchangeable.

reaction solutions are characterized by their ^{1}H-NMR spectra (400 MHz). In the case of the azo compound **5** only the diazetidine **8** is formed, that means without noticeable impurities ($\leq 1\%$). On the other hand, when irradiating **1** apart from the main product **6** described above additional signals are shown, which allows us to conclude the existence of small amounts of the diazetidine **7**. The reaction mixtures are worked up by preparative medium pressure chromatography (MPLC), which retains the product ratio of **6**:**7**. The experimental data are given below in Table 4.

Since compound **7** cannot be isolated purely it must be characterized merely by ^{1}H-NMR spectroscopy. In Table 5 the spectroscopical data of **7** are compared to those of the completely characterized compounds **1** (relative to the norbornene moiety) and **8** (relative to the diazetidine moiety). There is a very good agreement.

Irradiations in Methanol

Due to the bathochromic shift of the short-wavelength maximum of compound **1** in polar solvents irradiations were carried out at 254 nm in methanol. In that solvent it is possible to irradiate directly into the maximum of **1** at 252 nm by means of a low-pressure mercury lamp. According to the extinction coefficients shown by **2**, **3**, and **5**, it is expected that these compounds display photoreactivity, too, at 254 nm. The results of both, the irradiation experiments at 254 nm and the control experiments at 350 nm, are listed in Table 6.

Table 6. Irradiation experiments in methanol at 254 nm and 350 nm (Method B)

Compound	Time [min]	254-nm Product	Yield (MPLC)	Time [h]	350-nm Product	Yield (MPLC)
1	30	**6**:**7** (95:5)	80%	1	**6**:**7** (96:4)	94%
2	45	**9**	72%	5	**9**	90%
3	30	**10**	76%	2	**10**	90%
5	30	**8**	90%	4	**8**	90%

All experiments were carried out under exactly the same conditions and the products worked up using chromatography. The results can be summarized as follows:

1) Both, the excitation at 254 nm and the irradiation into the $n\pi^*$ transition at 350 nm, lead to the same reaction products. The product ratio of **6**:**7** of the irradiation of **1** hardly varies with the applied wavelength. In no case any by-products could be observed.

2) With long-wavelength irradiation the yields are slightly higher than at 254 nm. According to ^{1}H-NMR spectroscopical investigations **5** reacts quantitatively at 350 nm, but chromatography leads to losses of 5–10%.

3) The strikingly longer reaction times for the irradiation at 350 nm can be caused by different characteristics of the lamps and do not allow the conclusion of different quantum yields. However, considerably longer reaction times are found for the cyclization $\pi^6_{CC}-\pi_{NN}$ (**2**, **5**) than for $\pi^5_{CC}-\pi_{NN}$ (**1**, **3**).

Conclusion

According to the structure analysis of **1** the observed transanular distances agree satisfactorily with those calculated by the MNDO model. The distance $\pi^5_{CC}-\pi_{NN}$ is exactly the same as the corresponding separation in **3**[5]. The π_{NN} and π_{CC} units, respectively, are in a nearly perfect parallel orientation, which is shown by the interplanar angles of the C–C=C and C–N=N planes (8.8°, $\pi^5_{CC}-\pi_{NN}$; 15.0°, $\pi^6_{CC}-\pi_{NN}$).

Experimental

For general data of the employed equipment compare ref.[19]. Before each irradiation the glass equipment was cleaned with concentrated nitric acid and afterwards treated with concentrated ammonia.

For the preparation of the azo compounds **1**, **2**, **3**, and **5** compare ref.[4a]. In addition to the physical and analytical data described there both, UV spectra of the compounds **1**, **3**, and **5** (see Table 2) in different solvents and 400-MHz ^{1}H-NMR spectra of **1** and **5**, were recorded.

With reference to ref.[4a] the improved syntheses of *(t-4a,t-8a,t-9a,t-10a)-Δ⁶-dodecahydro-c-9,c-10-azo-r-1,c-4-etheno-t-5,t-8-methanoanthracene* (**1**) and *(t-4a,t-8a,t-9a,t-10a)-Δ⁶-dodecahydro-c-9,c-10-azo-r-1,c-4-etheno-c-5,c-8-methanoanthracene* (**5**) were carried out: 7.30 g (45.6 mmol) of the trimer (*c*-4a,*c*-8a)-4a,5,8,8a-tetrahydro-*r*-5,c-8-ethanophthalazine is treated with 150 ml of $CHCl_3$ and 41.0 g (0.46 mol) of norbornadiene. After adding dropwise 5.17 g of trifluoroacetic acid, the obtained solution is heated to 50°C for 24 h. Then the solution is transferred into a separatory funnel and is washed with saturated aqueous sodium hydrogen carbonate solution and with water. The organic layer is dried with K_2CO_3. After removing of the solvent under reduced pressure the residue is purified by flash-chromatography[20] (column: 40 × 3 cm; silica gel 32–63 μm (Woelm); EtOAc/petroleum ether, 1:1; UV detection at 380 nm). 3.70 g of a mixture of the isomeric azo compounds **1** and **5** is obtained, which can be separated by flash-chromatography (column: 30 × 3 cm, silica gel 32–63 μm (Woelm); EtOAc/CH_2Cl_2, 1:3; UV detection at 380 nm) into two portions of 1.85 g of the two components. In order to quicken the separation, compound **1** is eluted with a more polar eluent (EtOAc/CH_2Cl_2, 1:1). On the whole 620 mg (5%) of **1** and 2.57 g (22%) of **5** are obtained as slightly yellow or colourless crystals, respectively, which can be used for irradiation experiments after sublimation (120°C, 0.01 Torr).

1: ^{1}H NMR (400 MHz, $CDCl_3$): δ = 1.08 (*AA'*BB'MM', $J_{2\text{-}H,2\text{-}H'} = J_{3\text{-}H,3\text{-}H'}$ = 8.0 Hz, 2H; 2-H, 3-H), 1.13 (*A*B, $J_{11\text{-}H,11\text{-}H'}$ = 8.1 Hz, 1H; 11-H), 1.23 (A*B*, 1H; 11-H'), 1.40 (AA'*BB'*MM', 2H; 2-H', 3-H'), 2.02 (s, 2H; 4a-H, 9a-H), 2.34 (s, 2H; 8a-H, 10a-H), 2.43 (bs, 2H; 1-H, 4-H), 2.73 (pseudo-sept, *J* = 1.8 Hz, 2H; 5-H, 8-H), 4.92 (s, 2H; 9-H, 10-H); 5.31 (pseudo-t, *J* = 1.6 Hz, 2H; 6-H, 7-H), 5.66 (dd, *J* = 4.6 Hz, *J* = 3.1 Hz, 2H; 14-H, 15-H).

5: ^{1}H NMR (400 MHz, $CDCl_3$): δ = 0.83 (*AB*, $J_{11\text{-}H,11\text{-}H'}$ = 9.6 Hz, 1H; 11-H), 1.10 (*AA'*BB'MM', $J_{2\text{-}H,2\text{-}H'} = J_{3\text{-}H,3\text{-}H'}$ = 8.0 Hz, 2H, 2-H, 3-H), 1.27 (A*B*, 1H; 11-H'), 1.40 (AA'*BB'*MM', 2H; 2-H', 3-H'), 1.77 (s, 2H; 8a-H, 10a-H), 2.01 (s, 2H; 4a-H, 9a-H), 2.47 (bs, 2H; 1-H, 4-H), 2.72 (pseudo-quint, *J* = 1.7 Hz, 2H; 5-H, 8-H), 5.18 (s, 2H; 9-H, 10-H), 5.71 (dd, *J* = 4.7 Hz, *J* = 3.3 Hz, 2H; 14-H, 15-H), 6.02 (pseudo-t, *J* = 1.6 Hz, 2H; 6-H, 7-H).

The analytical and physical data of the photoproducts apart from compound **7** are described in ref.[4c]; in addition to that the 400-MHz ^{1}H-NMR spectra of **6**–**8** have been recorded.

(c-5a,c-9a)-Δ^7-Dodecahydro-r-6,c-9-ethano-t-1,t-5,t-2,t-4-(nitrilometheno)-1H-benzo[g]cyclopent[cd]indol (**6**): ^{1}H NMR (400 MHz, $CDCl_3$): δ = 1.25 (*AA'*BB'MM', 2H; 7-H, 8-H), 1.28 (*A*B, $J_{3\text{-}H,3\text{-}H'}$ = 11.1 Hz, 1H; 3-H), 1.51 (AA'*BB'*MM', 2H; 7-H', 8-H'), 1.78 (A*B*, 1H; 3-H'); 2.03 (s, 2H; 4a-H, 9c-H), 2.36 (s, 2H; 5a-H, 9a-H), 2.47 (b.s, 2H; 6-H, 9-H), 2.57 (pseudo-sept, *J* = 1.7 Hz, 2H; 2a-H, 4-H); 2.60 (s, 2H; 5-H, 9b-H), 4.15 (dd, *J* = 2.1 Hz, *J* = 3.4 Hz, 2H; 2-H, 13-H), 6.22 (dd, *J* = 3.2 Hz, *J* = 4.7 Hz, 2H; 10-H, 11-H).

(c-6a,c-10a)-Δ^8-Tetradecahydro-t-1,t-6,t-2,t-5-(nitrilometheno)-r-7,c-10-methanodibenz[cd,g]indol (**7**): ^{1}H NMR (400 MHz, $CDCl_3$): δ = 1.45 (pseudo-d, *J* = 8.1 Hz, 2H; 3-H, 4-H), 1.90 (pseudo-d, *J* = 8.1 Hz, 2H; 3-H', 4-H'), 2.31 (s, 2H; 5a-H, 10c-H), 2.45 (s, 2H; 6a-H, 10a-H), 2.61 (s, 2H; 6-H, 10b-H), 2.85 (s, 2H; 7-H, 10-H), 6.09 (pseudo-t, *J* = 1.6 Hz, 2H; 8-H, 9-H). – The diazetidine signals of 2-H, 13-H are covered by the corresponding signal of **6** (δ = 4.15). The expected AB multiplet of the methano bridge 11-H, 11-H' is presumably superimposed by the group of signals at δ = 1.25.

(t-6a,t-10a)-Δ^8-Tetradecahydro-c-1,c-6,c-2,c-5-(nitrilometheno)-r-7,c-10-methanodibenz[cd,g]indol (**8**): ^{1}H NMR ($CDCl_3$): δ = 1.21 (*AB*, $J_{11\text{-}H,11\text{-}H'}$ = 8.9 Hz, 1H; 11-H), 1.48 (*AA'*BB'MM', 2H; 3-H, 4-H), 1.74 (m, 2H; 6a-H, 10a-H), 1.78 (m_c, 2H; 2a-H, 5-H), 1.90 (AA'*BB'*MM', 2H; 3-H', 4-H'), 2.13 (A*B*, 1H; 11-H'), 2.31 (s, 2H; 5a-H, 10c-H), 2.69 (s, 2H; 6-H, 10b-H), 2.75 (pseudo-quint, *J* = 1.7 Hz, 2H; 7-H, 10-H), 4.17 (dd, *J* = 2.2 Hz, *J* = 3.4 Hz, 2H; 2-H, 13-H), 6.13 (pseudo-t, *J* = 1.7 Hz, 2H; 8-H, 9-H).

Method A. – Irradiations in $CDCl_3$ ($\lambda \geq 320$ nm): 30 mg of **1** or 45 mg of **5**, respectively, are dissolved in ca. 0.5 ml of $CDCl_3$ in an NMR tube. With the help of an adhesive tape the NMR tube is fixed at a pyrex immersion jacket, cooled to −20°C and irradiated by means of a mercury high-pressure lamp (Hanau TQ-150 W) until the reaction is complete. The reaction is followed by TLC (silica gel; CH_2Cl_2/MeOH/conc. NH_3, 100:10:1). At the end of the reaction the solvent is removed in vacuo, and the residue is purified by preparative medium pressure chromatography[21] [silica gel 15–25 μm (Merck); *N* = 4900; CH_2Cl_2/MeOH/conc. NH_3, 100:10:1; Diff. refractometer]. The identification of the reaction products was carried out by comparison of their spectra with those of authentical material.

Method B. – Irradiations in MeOH (254 nm and 350 nm): Solutions of 50.0 mg of each of the compounds **1**, **2**, **3**, and **5** in 60.0 ml of dry MeOH are irradiated in a quartz vessel of 100 cm length and ca. 120 ml volume (Rayonet RQV-118) under nitrogen. With the help of a water-cooled finger the inner temperature is kept at ca. 20°C. Reaction control and isolation of the products was carried out as described for method A. – Apparatus: Rayonet reactor[22]. Characteristics of the mercury low-pressure lamps used here: 254 nm: ca. 35 W; 1.65 × 10^{16} quanta/s/cm^3. 350 nm; ca. 24 W, (90% at 350 nm); 1.5–5 × 10^{16} quanta/s/cm^3.

X-ray Crystallography of **1**[18]

A clear, colourless crystal was optically centered on a Syntex four-circle diffractometer. The intensities of all reflections were measured according to the ω-technique (Mo-K_α, graphite monochromator) using a scan-range of 1° and a scan speed between 0.5 and 24.0 degrees min^{-1} as a function of the intensities of the reflections. In the range between 3.0° ≤ 2Θ ≤ 55° all reflections *hkl* with $F > 3\sigma(F)$ were applied for the structure determination. For the evaluation the SHELXTL system on an Eclipse S/250 computer was employed. The structure was solved by direct phase determination. The parameters of the complete structure could be refined by anisotropic least-squares cycles to the given *R* value. The positions of the hydrogen atoms were calculated geometrically and considered isotropically in all refinements. Special X-ray operations and results are listed below. Positional and thermal parameters of the atoms of **1** and bond lengths and angles are given in Tables 7 and 8, respectively.

Table 7. Atomic coordinates (× 10^4) and isotropic thermal parameters (pm^2 × 10^{-1}). The standard deviations are given in parentheses. The equivalent isotropic *U* is defined as one third of the trace of the orthogonalised U_{ij} tensor

	x	y	z	U
C(1)	2627(1)	-468(2)	-2267(4)	36(1)
N(2)	2833(1)	123(2)	-143(3)	38(1)
N(3)	2817(1)	1300(2)	-108(3)	39(1)
C(4)	2603(1)	1918(2)	-2198(4)	37(1)
C(5)	3085(1)	1495(2)	-3972(4)	38(1)
C(6)	3857(1)	1837(2)	-3835(4)	45(1)
C(7)	4187(1)	1347(3)	-1741(4)	46(1)
C(8)	4193(1)	95(3)	-1828(4)	46(1)
C(9)	3868(1)	-302(2)	-3987(4)	45(1)
C(10)	3090(1)	23(2)	-4047(4)	38(1)
C(11)	4105(1)	815(3)	-5422(4)	54(1)
C(12)	1899(1)	-28(2)	-2927(4)	35(1)
C(13)	1887(1)	1445(2)	-2926(4)	35(1)
C(14)	1284(1)	1912(2)	-1598(4)	45(1)
C(15)	1326(1)	1318(3)	626(4)	53(1)
C(16)	1345(1)	81(3)	642(4)	53(1)
C(17)	1317(1)	-536(2)	-1568(4)	43(1)
C(18)	648(1)	-83(3)	-2726(4)	52(1)
C(19)	630(1)	1383(3)	-2758(4)	52(1)

Table 8. Bond lengths [pm] and bond angles [deg]. The standard deviations are given in parentheses

C(1)	– N(2)	148.9(3)	N(2)	– C(1)	– C(10)	109.8(2)
C(1)	– C(10)	154.7(3)	N(2)	– C(1)	– C(12)	108.6(2)
C(1)	– C(12)	154.0(3)	C(10)	– C(1)	– C(12)	106.3(2)
N(2)	– N(3)	124.0(3)	C(1)	– N(2)	– N(3)	115.3(2)
N(3)	– C(4)	148.6(3)	N(2)	– N(3)	– C(4)	115.4(2)
C(4)	– C(5)	154.4(3)	N(3)	– C(4)	– C(5)	109.2(2)
C(4)	– C(13)	154.0(3)	N(3)	– C(4)	– C(13)	109.3(2)
C(5)	– C(6)	155.7(3)	N(5)	– C(4)	– C(13)	106.4(2)
C(5)	– C(10)	155.0(3)	C(4)	– C(5)	– C(6)	121.4(2)
C(6)	– C(7)	150.9(4)	C(4)	– C(5)	– C(10)	108.3(2)
C(6)	– C(11)	154.7(4)	C(6)	– C(5)	– C(10)	103.0(2)
C(7)	– C(8)	132.0(4)	C(5)	– C(6)	– C(7)	110.4(2)
C(8)	– C(9)	151.0(4)	C(5)	– C(6)	– C(11)	98.0(2)
C(9)	– C(10)	156.4(3)	C(7)	– C(6)	– C(11)	99.7(2)
C(9)	– C(11)	155.6(4)	C(6)	– C(7)	– C(8)	108.1(2)
C(12)	– C(13)	155.1(3)	C(7)	– C(8)	– C(9)	107.9(2)
C(12)	– C(17)	154.3(3)	C(8)	– C(9)	– C(10)	109.6(2)
C(13)	– C(14)	154.9(3)	C(8)	– C(9)	– C(11)	99.6(2)
C(14)	– C(15)	150.6(4)	C(10)	– C(9)	– C(11)	98.0(2)
C(14)	– C(19)	154.6(3)	C(1)	– C(10)	– C(5)	108.0(2)
C(15)	– C(16)	130.2(4)	C(1)	– C(10)	– C(9)	121.0(2)
C(16)	– C(17)	150.8(4)	C(5)	– C(10)	– C(9)	103.1(2)
C(17)	– C(18)	154.2(3)	C(6)	– C(11)	– C(9)	93.1(2)
C(18)	– C(19)	154.3(4)	C(1)	– C(12)	– C(13)	108.3(2)
			C(1)	– C(12)	– C(17)	117.0(2)
			C(13)	– C(12)	– C(17)	109.5(2)
			C(4)	– C(13)	– C(12)	108.0(2)
			C(4)	– C(13)	– C(14)	117.0(2)
			C(12)	– C(13)	– C(14)	109.2(2)
			C(13)	– C(14)	– C(15)	109.8(2)
			C(13)	– C(14)	– C(19)	106.3(2)
			C(15)	– C(14)	– C(19)	106.3(2)
			C(14)	– C(15)	– C(16)	115.0(2)
			C(15)	– C(16)	– C(17)	115.1(2)
			C(12)	– C(17)	– C(16)	110.1(2)
			C(12)	– C(17)	– C(18)	106.1(2)
			C(16)	– C(17)	– C(18)	106.3(2)
			C(17)	– C(18)	– C(19)	109.5(2)
			C(14)	– C(19)	– C(18)	109.6(2)

Empirical formula: $C_{17}H_{20}N_2$ (252.36); crystal size: 1.0 × 1.5 × 0.4 mm; number of measured intensities: 3125; number of observed

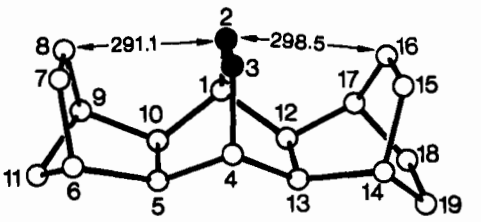

Figure 5. Perspective drawing of **1** with the labeling of the atoms corresponding to Tables 7 and 8. White and black spheres represent carbon and nitrogen atoms, respectively. Two nonbonding NC distances are inscribed

reflections: 2519; number of structure factors of direct phase determination: 420; R_{aniso} = 0.073; space group = $P2_1/a$ (14); cell parameters: a = 1964.7(12), b = 1052.7(5), c = 616.5(5) pm, β = 92.56(5)°; Z = 4; d_c = 1.316 g · cm^{-3}. Number of refined parameters: 173. Residual electron density: 0.464 e/Å^3.

CAS Registry Numbers

1: 89771-88-0 / **2**: 89703-54-8 / **3**: 63904-59-6 / **5**: 89703-58-2 / **6**: 90213-94-8 / **7**: 105879-76-3 / **8**: 90213-97-1 / **9**: 90213-95-9 / **10**: 63904-60-9 / (*c*-4a,*c*-8a)-4a,5,8,8a-tetrahydro-*r*-5,*c*-8-ethanophthalazine: 105786-52-5 / Norbornadiene: 121-46-0

[1] *Small and Medium Rings*, Part 63. – Part 62: E. Honegger, E. Heilbronner, N. Heß, H. D. Martin, *Chem. Ber.* **120** (1987) 187, preceding.

[2] M. J. Goldstein, R. Hoffmann, *J. Am. Chem. Soc.* **93** (1971) 6193.

[3] E. Haselbach, E. Heilbronner, G. Schröder, *Helv. Chim. Acta* **54** (1971) 153.

[4] [4a] S. Hünig, F. Prokschy, *Chem. Ber.* **117** (1984) 534. – [4b] W. Berning, S. Hünig, F. Prokschy, *Chem. Ber.* **117** (1984) 1455. – [4c] B. Albert, W. Berning, C. Burschka, S. Hünig, F. Prokschy, *Chem. Ber.* **117** (1984) 1465.

[5] B. Albert, W. Berning, C. Burschka, S. Hünig, H. D. Martin, F. Prokschy, *Chem. Ber.* **114** (1981) 423; **115** (1982) 402.

[6] K. Beck, S. Hünig, G. Kleefeld, H. D. Martin, K. Peters, F. Prokschy, H. G. v. Schnering, *Chem. Ber.* **119** (1986) 543.

[7] P. Bischof, J. A. Hashmall, E. Heilbronner, V. Hornung, *Helv. Chim. Acta* **52** (1969) 1745.

[8] M. J. S. Dewar, W. Thiel, *J. Am. Chem. Soc.* **99** (1977) 4899; W. Thiel, *QCPE*, Nr. 438.

[9] N. L. Allinger, M. T. Tribble, M. A. Miller, D. H. Wertz, *J. Am. Chem. Soc.* **93** (1971) 1637.

[10] D. C. Crans, J. P. Snyder, *Chem. Ber.* **113** (1980) 1201.

[11] R. C. Bingham, M. J. S. Dewar, D. H. Lo, *J. Am. Chem. Soc.* **97** (1975) 1285.

[12] L. Asbrink, C. Fridh, E. Lindholm, *Chem. Phys. Lett.* **52** (1977) 69, 72, *QCPE*, Nr. 393.

[13] W. J. Hehre, R. F. Stewart, J. A. Pople, *J. Chem. Phys.* **51** (1969) 2657.

[14] C. Santiago, E. J. McAlduff, K. N. Houk, R. A. Snow, L. A. Paquette, *J. Am. Chem. Soc.* **100** (1978) 6149.

[15] E. Osawa, K. Aigami, Y. Inamoto, *J. Org. Chem.* **42** (1977) 2621.

[16] J. Del Bene, H. H. Jaffé, *J. Chem. Phys.* **48** (1968) 1807; H. H. Jaffé, *QCPE*, Nr. 315.

[17] M. J. Mirbach, Kou-Chang Lui, M. F. Mirbach, W. R. Cherry, N. J. Turro, P. S. Engel, *J. Am. Chem. Soc.* **100** (1978) 5122.

[18] Further details of the structure determination are deposited at the Fachinformationszentrum Energie, Physik, Mathematik, D-7514 Eggenstein-Leopoldshafen (FRG). These data are available with quotation of the registry number CSD 51709, the authors, and the reference to this publication.

[19] K. Beck, A. Höhn, S. Hünig, F. Prokschy, *Chem. Ber.* **117** (1984) 517.

[20] W. C. Still, M. Kahn, A. Mitra, *J. Org. Chem.* **43** (1978) 2923.

[21] *MPLC (Medium Pressure Liquid Chromatography)* according to G. Helmchen and B. Glatz, Privatdruck, Stuttgart 1978.

[22] The Southern New England Ultraviolet Co., 55 Connolly Parkway Hamden, Connecticut, U.S.A. 06514.

[207/86]